

Bose-Hubbard lattice as a controllable environment for open quantum systems

Francesco Cosco,¹ Massimo Borrelli,¹ Juan José Mendoza-Arenas,^{2,3}
Francesco Plastina,^{4,5} Dieter Jaksch,^{3,6} and Sabrina Maniscalco^{1,7}

¹*Turku Centre for Quantum Physics, Department of Physics and Astronomy,
University of Turku, FI-20014 Turun yliopisto, Finland*

²*Departamento de Física, Universidad de los Andes, A.A. 4976, Bogotá D. C., Colombia*

³*Clarendon Laboratory, University of Oxford, Parks Road, Oxford OX1 3PU, United Kingdom*

⁴*Dipartimento di Fisica, Università della Calabria, 87036, Arcavata di Rende (CS), Italy*

⁵*INFN - Gruppo Collegato di Cosenza, Cosenza, Italy*

⁶*Centre for Quantum Technologies, National University of Singapore, 3 Science Drive 2, Singapore 117543*

⁷*Center for Quantum Engineering, Department of Applied Physics,
Aalto University School of Science, P.O. Box 11000, FIN-00076 Aalto, Finland*

We investigate the open dynamics of an atomic impurity embedded in a one-dimensional Bose-Hubbard lattice. We derive the reduced evolution equation for the impurity and show that the Bose-Hubbard lattice behaves as a tunable engineered environment allowing to simulate both Markovian and non-Markovian dynamics in a controlled and experimentally realisable way. We demonstrate that the presence or absence of memory effects is a signature of the nature of the excitations induced by the impurity, being delocalized or localized in the two limiting cases of superfluid and Mott insulator, respectively. Furthermore, our findings show how the excitations supported in the two phases can be characterized as information carriers.

Introduction - Several condensed matter models have been recently investigated from an open system viewpoint. Typically, one imagines embedding an impurity in a much larger many-body system that acts as its environment. The underlying idea is that, by monitoring dynamical properties of such a probe-impurity, one can access information about the many-body system indirectly and, ideally, with very little disturbance. Several features of a many-body system can be thoroughly investigated within this framework, from single-particle excitation spectra to many-body correlations [1–5].

In a complementary fashion, one can shift the perspective and study properties of the impurity dynamics itself. In this respect, an interesting question to ask is whether the open dynamics induced by a many-body system is memoryless or not. Generally, the answer depends on the specific system at hand, as well as on those controllable parameters that make tunable the many-body environment. Open system dynamics induced in many-body experimental platforms have been studied and simulated mainly in the Markovian, or memory-free, regime [6–9], modelled by a Lindblad master equation [10]. In a number of physical scenarios, however, a Markovian description of the dynamics is inadequate [11–13]. Furthermore, memory effects may be beneficial for certain quantum-enhanced protocols, such as superdense coding [14, 15], teleportation [16], and quantum key-distribution [17], and they play a key role as well in quantum thermodynamics [18] and measurement theory [19]. Their quantification in terms of information backflow has led to the introduction of a number of non-Markovianity measures or witnesses, based on the dynamical properties of different quantum information quantifiers [20–25]. Depending on both the system and the quantum protocol of interest, one may choose the appropriate non-Markovianity measure and investigate if and in which way memory effects lead to optimised performance. In light of this renewed interest in non-Markovian dynamics, a

few experiments in the quantum optical domain have been performed to implement quantum simulators of simple non-Markovian models [26–34]. At the same time a number of theoretical studies have demonstrated that many-body environments may induce memory effects in the dynamics of an interacting impurity [35–40].

In this Letter, we focus on the Bose-Hubbard model, which is efficiently implemented using cold atoms in optical lattices [41–43]. In particular, the occurrence of a critical point has been demonstrated, which separates a superfluid quasi-condensate from a Mott insulator phase [44]. We consider the one-dimensional model, whose phase diagram has been extensively investigated [45]. In contrast to previous works on spin system and ion crystals [46, 47], our results show for the first time the existence of a direct connection between the presence or absence of memory effects in the induced open system dynamics and the nature of the environmental excitations, giving rise to either delocalized or localized density fluctuations in the two phases, respectively. By using both analytical and numerical tools, we evaluate the amount of information backflow and its dependence upon the parameters of the Bose-Hubbard model. In particular, we adopt two different analytic approaches in the superfluid and deep Mott regimes, respectively, which allowed us to identify the single particle excitations in the two phases and to obtain their contributions to information flow and memory effects. Then we use numerical t-DMRG to interpolate between the two extremes and analyse non-Markovianity close to the transition point. Besides directly linking memory effects to the physical properties of the information carriers, this analysis offers the possibility of characterizing the mobility of the excitations from a quantum information perspective.

In a related work [67], memory effects induced by Anderson localisation were studied for a two-level atom coupled to a one-dimensional array of disordered cavities, and

non-Markovianity was shown to increase with the disorder strength. Taken together with these observations, our results point towards a possible universal connection between non-Markovianity and localization in complex many-body environments.

Impurity dephasing in the Bose-Hubbard lattice - The dynamics of a cold gas of bosonic atoms trapped in a one-dimensional optical lattice and confined to the lowest Bloch band is governed by the Bose-Hubbard Hamiltonian [41, 48]

$$\hat{H}_{BH} = -J \sum_i (\hat{a}_i^\dagger \hat{a}_{i+1} + \hat{a}_{i+1}^\dagger \hat{a}_i) + \frac{U}{2} \sum_i \hat{n}_i (\hat{n}_i - 1), \quad (1)$$

where J is the hopping parameter, U is the localising on-site interaction, $\hat{a}_i, \hat{a}_i^\dagger$ are the standard boson annihilation and creation operators and $\hat{n}_i = \hat{a}_i^\dagger \hat{a}_i$. In the limits $J = 0$ and $U = 0$, the above Hamiltonian is exactly solvable, with the ground states describing either a Mott insulator, with a uniform occupation number per site \bar{n} , or a quasi-condensate, with a macro-occupancy of the lowest momentum-state, respectively. The intermediate regime is analytically intractable but approximate models can be employed in the $J \gg U$ and $U \gg J$ regimes [49–51].

A single atomic impurity can be used to investigate features of the lattice trapped gas [52–54]. We assume that the impurity is harmonically confined in three dimensions, frozen in its motional ground state, whose wavefunction is a Gaussian centered at a specific site (say $i = 0$) of the lattice. This setting can be practically implemented using selective optical potentials that are able to confine different internal states or different atomic species independently [55–60]. The impurity and the surrounding gas are coupled via a density-density interaction, whose strength depends on the internal state of the impurity, and which couples it to the local number operator \hat{n}_0 [1, 61]. We assume that only the two lowest internal levels of the impurity ($|e\rangle, |g\rangle$) are relevant to the dynamics and that $|g\rangle$ does not couple to the gas. This can be achieved by a Feshbach resonance [55–61]. The total Hamiltonian reads $\hat{H} = \frac{\omega_0}{2} \hat{\sigma}_z + \hat{H}_{BH} + U_e |e\rangle\langle e| \otimes \hat{n}_0$, where U_e is an effective coupling constant accounting for the spatial overlap between the impurity and the gas wave functions. We will consider a repulsive interaction, $U_e > 0$.

Starting with the impurity initially in state $|g\rangle$, we assume it to be transferred into an equal superposition of $|g\rangle$ and $|e\rangle$ by a $\pi/2$ pulse. The ensuing evolution generated by \hat{H} will not lead to population transfer. It will, however, cause dephasing, giving rise to a decay of the impurity coherence. The central physical quantity of interest in this work will be the decoherence function, which we will use to characterize the impurity dynamics. It can be measured in a Ramsey-type experiment by applying a second $\pi/2$ pulse, after a variable delay t , that maps the relative phase between $|g\rangle$ and $|e\rangle$ into a measurable population imbalance [62]. The environment-induced dynamics of the impurity's internal levels can be either memory-less (Markovian), with a monotonic loss of the initial coherence, or with memory (non-Markovian), with some temporary and partial recovery. Starting from the microscopic Hamiltonian \hat{H} ,

by means of standard time convolutionless projection operator technique [63], one can derive a perturbative master equation for the reduced impurity state,

$$\frac{d\rho}{dt} = -\frac{i\bar{\omega}_0}{2} [\hat{\sigma}_z, \rho] + \gamma(t) (\hat{\sigma}_z \rho \hat{\sigma}_z - \rho), \quad (2)$$

which is well known as a dephasing master equation (with a renormalized transition frequency $\bar{\omega}_0$). The time-dependent transition rate $\gamma(t)$ is directly connected to the density fluctuations of the gas

$$\gamma(t) = U_e^2 \text{Re} \int_0^t dt' \langle \hat{n}_0(t') \hat{n}_0(0) \rangle. \quad (3)$$

Through this relation, the properties of the Bose-Hubbard gas are dynamically mapped into the impurity time evolution, which comes out to be Markovian if and only if the decay rate is positive at all times, implying no memory-effects. Non-Markovian dynamics occurs, instead, if at least one time interval exists for which $\gamma(t) < 0$, causing information back-flow [21]. This is directly linked to the time behaviour of the Loschmidt echo, defined as $L(t) \equiv |\langle \phi(t) | \phi'(t) \rangle|^2$, with $|\phi(t)\rangle$ being the ground state $|\phi(0)\rangle$ of \hat{H}_{BH} , chosen as the initial state, evolved according to \hat{H}_{BH} only, while $|\phi'(t)\rangle$ is the time-evolved state in the presence of the impurity. It turns out that $|\rho_{eg}(t)|/|\rho_{eg}(0)| = |\langle \phi(0) | e^{i\hat{H}_g t} e^{-i\hat{H}_e t} | \phi(0) \rangle| = \sqrt{L(t)}$, where $\hat{H}_k = \langle k | \hat{H} | k \rangle$, with $k = g, e$. Therefore, $\sqrt{L(t)} = e^{\Gamma(t)}$, where $\Gamma(t) = -\int_0^t dt' \gamma(t')$, is uniquely determined by the dephasing coefficient of the impurity.

In order to investigate the Markovian or non-Markovian character of the dynamics induced by the engineered quantum environment we use the trace-distance measure (BLP measure) quantifying information flow in terms of distinguishability between two arbitrary quantum states of the probe [21]. It is worth stressing that, for the open quantum system investigated here, all non-Markovianity measures agree in discerning Markovian from non-Markovian dynamics [10, 64]. For our case, the BLP non-Markovianity measure \mathcal{N} can be explicitly computed via the Loschmidt echo [46, 65]

$$\mathcal{N} = \sum_n \sqrt{L(t_{n+1})} - \sqrt{L(t_n)}, \quad (4)$$

where the sum is taken over the set of time intervals $[t_n, t_{n+1}]$ at which the echo increases. During these intervals, some of the previously lost information regarding the state of the impurity is temporarily recovered, thanks to the fact that the dephasing coefficient $\gamma(t)$ becomes temporarily negative.

Dephasing dynamics in the limiting cases - We assume the total system to be initially at zero temperature, with the gas prepared in its ground state, and the impurity in an equal superposition state. In the superfluid regime, $U \ll J$, the kinetic energy of the atoms in the lattice is much larger than the on-site interaction, and hence the latter can be treated as a weak perturbation. The gas is a 1D quasi-condensate whose majority of atoms occupy the $k = 0$ momentum state. It can

be described using Bogoliubov mean-field theory [49], which allows us to recast the local density operator as follows

$$\hat{n}_0 = n_0 + \sum_k \frac{\beta_k}{N_s} (\hat{b}_k^\dagger + \hat{b}_k), \quad (5)$$

in which n_0 is the condensate density, $\beta_k = \sqrt{n_0 N_s} (u_k + v_k)$ is the spectral density expressed in terms of the Bogoliubov coefficients u_k, v_k [49], and \hat{b}_k^\dagger create the Bogoliubov quasi-particle excitations with momentum k (with N_s being the number of lattice sites). In the strongly interacting regime $U \gg J$, we use the doublon-holon approximate description instead, derived in [50, 51] and successfully employed to study out-of-equilibrium dynamics [68]. We assume that, if the gas filling factor is \bar{n} , defining the ground state $|\text{GS}\rangle \propto \otimes_j |\bar{n}\rangle_j$ in the limit $U/J \rightarrow \infty$, then only the local states $|\bar{n}\rangle$, $|\bar{n} + 1\rangle$ and $|\bar{n} - 1\rangle$ play a major role in the dynamics. Truncating the local basis to these three states [51], we obtain an effective description of the system in terms of fermionic excitations, giving

$$\hat{n}_0 = \bar{n} + \frac{1}{N_s^2} \sum_{k,q} \cos\left(\frac{\theta_k - \theta_q}{2}\right) (\hat{d}_k^\dagger \hat{d}_q - \hat{h}_k^\dagger \hat{h}_q) + i \sin\left(\frac{\theta_k - \theta_q}{2}\right) (\hat{d}_k^\dagger \hat{h}_{-q}^\dagger - \hat{h}_{-q} \hat{d}_k), \quad (6)$$

where \hat{d}_k^\dagger (\hat{d}_k) and \hat{h}_k^\dagger (\hat{h}_k) are fermionic operators creating (destroying) doublon and holon excitations, respectively [76]. This approach breaks down for $U/J < 4(\bar{n} + 1)$, therefore choosing $\bar{n} = 1$ restricts the range of validity to $U/J \geq 8$.

In the two limiting cases, analytic expressions for the dephasing rate can be derived by plugging the density fluctuations of (5) and (6) into the expression for $\gamma(t)$. Including the constant density component in the unitary evolution, and taking the average over the respective vacuum states, we obtain:

$$\gamma_{SF}(t) = U_e^2 \sum_k \frac{|\beta_k|^2}{N_s^2} \left(\frac{\sin \omega_k t}{\omega_k} \right), \quad (7)$$

$$\gamma_M(t) = U_e^2 \sum_{k,q} \sin^2\left(\frac{\theta_k - \theta_q}{2}\right) \frac{\sin(\omega_k^d + \omega_q^h)t}{N_s^2(\omega_k^d + \omega_q^h)}, \quad (8)$$

where ω_k and $\omega_k^{d/h}$ are the energies of the superfluid and doublon/holon excitations, respectively [77]. As we discuss below, while γ_{SF} gives rise to a purely Markovian impurity dynamics (due to delocalised excitations), γ_M results in a generally non-zero information backflow (due to the doublon-holon pairs, generating localised particle density fluctuations).

Results - As seen from Eq. (4), non-Markovian effects occur if the Loschmidt echo does not decay monotonically (requiring a temporary negative $\gamma(t)$). In the superfluid regime, $L(t)$ displays revivals at long times only, due to finite size effects, see panel (a) of Fig. 1. The memory-inducing mechanism, in this case, is the following: after the impurity is embedded in the Bose lattice at site 0, representing the center of the lattice, the repulsion generates a small depletion of the quenched site, and a fraction of the initial particles moves

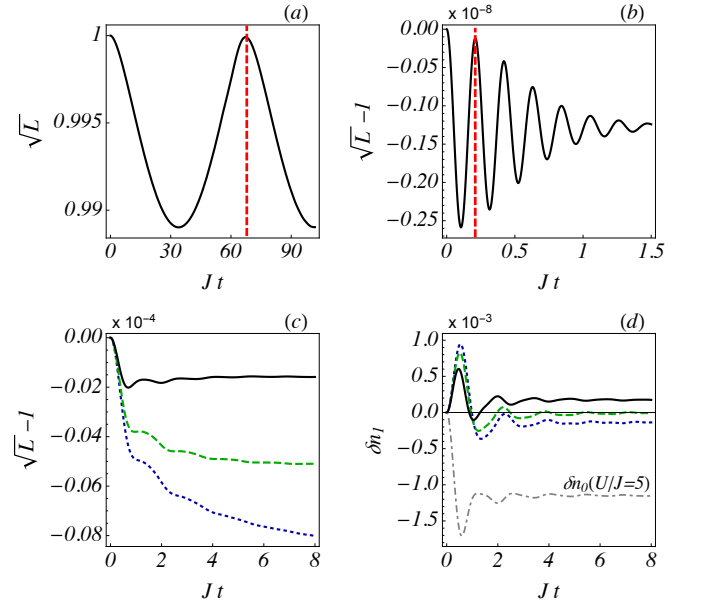


Figure 1. (Color online). (a): Loschmidt echo in the superfluid phase calculated using Eq. (7) at $U/J = 1$, the vertical line is the recurrence time $\tau = \frac{N_s}{c_s} \approx \frac{2\pi}{\omega_{k=2\pi/N_s}}$, due to finite size effects. (b): Loschmidt echo deep in the insulating phase at $U/J = 30$, the vertical line is $\tau = \frac{2\pi}{U}$. (c): Loschmidt echo in the intermediate regime for $U/J = 3.5, 4, 5$ in dotted blue, dashed green and solid black, respectively. (d): density fluctuations in the nearest neighbor of the quenched site (dubbed as 1) for $U/J = 3.5, 4, 5$ in dotted blue, dashed green and solid black, respectively. The dot-dashed gray line gives the density fluctuation in the perturbed site for $U/J = 5$. In all the panels $U_e/J = 0.01$ and $N_s = 96$. Data displayed in (b), (c) and (d) were obtained through particle-conserving ($\bar{n} = 1$) t-DMRG calculations.

towards the neighbouring sites. In the superfluid regime, a density wave is generated, which travels freely throughout the lattice. Revivals in the density of the quenched site (and, as a consequence, in the Loschmidt echo) are due to this wave reaching the boundary - because of the finite size - and bouncing back towards its source. In the Bogoliubov mean field approach, delocalised phononic excitations have the effective speed of sound $c_s = \sqrt{2JU n_0}$, so that we can predict the revival time to be N_s/c_s .

In the Mott phase, the behaviour is qualitatively different. At strong interactions, the energy of a pair of two distinct types of quasiparticle with opposite momenta is $2\Omega(k) \approx U - 2J(2\bar{n} + 1)\cos k$ [51, 77]. In this regime, the maximal relative velocity of a pair is found at $|k| \approx \frac{\pi}{2}$, where the spectral density exhibits a maximum. As a result, the decoherence function shows the first revival at $t \approx \frac{2\pi}{2\Omega(\pi/2)} = \frac{2\pi}{U}$, in agreement with the numerics, see panel (b) of Fig. 1. Hence, the non-monotonicity of the Loschmidt echo occurs for shorter and shorter times with increasing the interaction strength. In the limit $U/J \rightarrow \infty$, the gas approaches the hard-core boson limit, with the exact eigenstates of the Hamiltonian in Eq. (1) being given by local Fock states $|n\rangle_j$. In this case, the interaction with the impurity only causes a local energy shift, gener-

ating no dynamics and no memory effects at all.

Around the critical point $(U/J)_c \approx 3.4$ [71–73], the description gets more involved as mean field approaches do not hold anymore. In analogy to the limiting cases discussed above, we can start off considering the effect of the impurity on the local particle density. As expected, a depletion of the quenched site occurs; however, the local density displays a few oscillations only, before reaching a stationary value. In the Mott phase, the response of the gas after the embedding of the impurity can be witnessed by analysing the density fluctuations at the neighbouring site $i = 1$, $\delta n_1(t) = \langle \hat{n}_1(t) \rangle - \langle \hat{n}_1 \rangle_{\text{GS}}$. For $U/J \lesssim 4$, after a quick transient with a positive density fluctuation, a negative stationary value is reached, see panel (d) of Fig. 1. After $U/J \approx 4$ the extra particles moving away from site 0 stay almost localized, as they oscillate back and forth, accumulating (on average) on site 1, i.e. generating a positive stationary value for the density fluctuation.

To understand this behavior, we can compare it with the results of Ref. [74], where the expansion velocity v_c of an initially held cloud of atoms in a 1D Bose-Hubbard lattice was thoroughly investigated and a minimum was found at $(U/J)_{v_c} \simeq 4$, consistently with other experimental observations [75]. In that scenario, high occupancy states begin to form at small U/J (but still in the Mott phase), resulting in a reduction of the expansion velocity of the cloud. In our setup, where the lattice is not switched off, the excess of particles generated by the impurity ends up trapped in the vicinity of the quenched site for $U/J \gtrsim 4$. In the intermediate regime (between the critical point and $U/J \simeq 4$), instead, they are able to propagate even though the environment has entered the insulating phase. This behaviour can be related to the emergence of structures in the Loschmidt echo. Proper oscillations are found for $U \gtrsim 4$, with $L(t)$ displaying a series of maxima and minima that signal a non-Markovian dynamics, ultimately due to the localized character of the density fluctuations, see panel (c) in Fig. 1. On the other hand, for $U \lesssim 4$ the Loschmidt echo displays a series of inflection points, not giving rise to any true memory effect. Finally, all these structures disappear in the superfluid regime.

The memory quantifier displays the counterpart of these different behaviours of the local density. In Fig. 2, we display the normalized non-markovianity measure, $\bar{N} = N/N_{\text{max}}$, comparing a numerical calculation with the analytic results obtained with the doublon-holon model in the thermodynamic limit [70]. The plot summarises our findings, showing that the two limiting phases of the lattice gas are characterised by qualitatively different dynamics: fully Markovian when the environment is in the superfluid phase and non-Markovian when the environment is deep in the Mott insulator phase. The Markovian-to-non-Markovian transition occurs at $(U/J)_{\bar{N}} \simeq 4$, different from but still quite close to the critical point. Notice, in particular, the good agreement between the numerical and the approximate analytic results, discrepancies being due to the perturbative nature of the master equation and to the truncation of the Hilbert space adopted in the analytic approach. Increasing the ratio U/J , the two

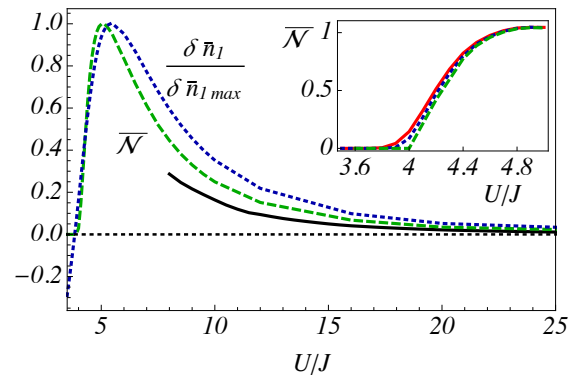


Figure 2. (color online): Comparison between numerical (dashed green, $N_s = 96$) and analytical (solid black, $N_s \rightarrow \infty$) normalized non-Markovianity measure $\bar{N} = N/N_{\text{max}}$ and average excess particle number at site 1, $\delta \bar{n}_1 / \delta \bar{n}_{1\text{max}}$ (dotted blue, $N_s = 96$), where the time average is performed over $JT = 2\pi$. In the inset, \bar{N} for different lattice sizes, $N_s = 80, 96$ and 128 in solid red, dotted blue and dashed green respectively.

calculation methods agree in giving an amount of information backflow that decays asymptotically to zero. The onset of non-Markovian dynamics is then compared with the time averaged occupancy fluctuation of the impurity’s adjacent site $\delta \bar{n}_1 = 1/T \int_0^T \langle \hat{n}_1(t) \rangle - \langle \hat{n}_1 \rangle_{\text{GS}}$. This quantity is negative for values of U/J at which the gas has a larger mobility, resulting in quasi-particles being pushed away from the neighbourhood of the impurity and spreading without any backflow, hence leading to Markovian dynamics. As soon as $\delta \bar{n}_1$ becomes positive, extra particles moving away from site 0 oscillate back and forth, accumulating (on average) on site 1, and giving rise to the observed memory effects. This is true up to a maximum after which the gas approaches the hard-core boson limit, where even these oscillations are strongly suppressed, resulting in a decay of $\delta \bar{n}_1$ back to its ground-state value, and in a tendency of the dynamics to become memoryless again. In this system, therefore, we can understand the quasi-particles as the physical information carriers, their dynamics being uniquely connected to information backflow and non-Markovian memory effects.

Conclusions and outlook - We have investigated the open system dynamics induced by a Bose-Hubbard lattice when it plays the role of environment for an (open) impurity system. We have derived the generalized master equation for the open system dynamics and linked the dephasing coefficient to the density-density correlations of the cold atom environment. Using both analytical and numerical techniques we have studied the non-equilibrium dynamics of the total system and we have shown that the ratio U/J can be thought of as a control parameter allowing to manipulate the nature of the information carriers and thus ruling the Markovian to non-Markovian crossover. In this sense, the Bose-Hubbard lattice can act as a controllable engineered environment, allowing for the simulation of open quantum system dynamics in both Markovian and non-Markovian regimes. We have shown that in this system

the presence or absence of memory effects is directly linked to the nature of the excitations induced in the environmental ground state and showed how the onset of memory effects signals the trapping of higher occupancies in the vicinity of the impurity.

Acknowledgements- The authors acknowledge support from the Horizon 2020 EU collaborative projects QuProCS (Grant Agreement No. 641277). D. J. acknowledges EPSRC support by projects EP/P009565/1 and EP/K038311/1. The authors also acknowledge the use of the University of Oxford Advanced Research Computing (ARC) facility in carrying out this work. <http://dx.doi.org/10.5281/zenodo.22558>. This research is partially funded by the European Research Council under the European Unions Seventh Framework Programme (FP7/2007-2013)/ERC Grant Agreement no. 319286 Q-MAC. This work was also supported by the EPSRC National Quantum Technology Hub in Networked Quantum Information Processing (NQIT) EP/M013243/1. J. J. M. A. acknowledges financial support from Facultad de Ciencias at UniAndes-2015 project Quantum control of non-equilibrium hybrid systems-Part II.

-
- [1] M. Bruderer and D. Jaksch, *New J. Phys.* **8**, 87 (2006).
- [2] A. Kantian, U. Schollwock, and T. Giamarchi, *Phys. Rev. Lett.* **115**, 165301 (2015).
- [3] M. T. Mitchison, T. H. Johnson, D. Jaksch, *Phys. Rev. A* **94**, 063618 (2016).
- [4] T. J. Elliott, T. H. Johnson, *Phys. Rev. A* **93**, 043612 (2016).
- [5] M. Streif, A. Buchleitner, D. Jaksch, J. Mur-Petit, *Phys. Rev. A* **94**, 053634 (2016).
- [6] S. Maniscalco, J. Piilo, F. Intravaia, F. Petruccione, and A. Messina, *Phys. Rev. A* **69**, 052101 (2004).
- [7] J. T. Barreiro, M. Miller, P. Schindler, D. Nigg, T. Monz, M. Chwalla, M. Hennrich, C. F. Roos, P. Zoller, and R. Blatt, *Nature* **470**, 486-491 (2011).
- [8] P. Schindler, M. Miller, D. Nigg, J. T. Barreiro, E. A. Martinez, M. Hennrich, T. Monz, S. Diehl, P. Zoller, and R. Blatt, *Nat. Phys.* **9**, 361-367 (2013).
- [9] H. Weimer, M. Miller, I. Lesanovsky, P. Zoller, and H. P. Buchler, *Nat. Phys.* **6**, 382 (2010).
- [10] H.-P. Breuer, E.-M. Laine, J. Piilo, and B. Vacchini, *Rev. Mod. Phys.* **88**, 021002 (2016).
- [11] F. Jelezko, T. Gaebel, I. Popa, A. Gruber, and J. Wrachtrup, *Rev. Mod. Phys.* **92**, 076401 (2016).
- [12] E. Paladino, Y.M. Galperin, G. Falci, and B.L. Altshuler, *Rev. Mod. Phys.* **86**, 361 (2014).
- [13] N. Vats and S. John, *Phys. Rev. A* **58**, 4168 (1998).
- [14] A. Karlsson, H. Lyyra, E.-M. Laine, S. Maniscalco, and J. Piilo, *Phys. Rev. A* **93**, 032135 (2016).
- [15] B.-H. Liu, X.-M. Hu, Y.-F. Huang, C.-F. Li, G.-C. Guo, A. Karlsson, E.-M. Laine, S. Maniscalco, C. Macchiavello, and J. Piilo, *EPL* **114**, 10005 (2016).
- [16] E.-M. Laine, H.-P. Breuer, and J. Piilo, *Sci. Rep.* **4**, 4620 (2014).
- [17] R. Vasile, S. Olivares, M. G. A. Paris, and S. Maniscalco, *Phys. Rev. A* **83**, 042321 (2011).
- [18] B. Bylicka, M. Tukiainen, D. Chruściński, J. Piilo, and S. Maniscalco, *Sci. Rep.* **6**, 27989 (2016).
- [19] G. Karpat, J. Piilo, and S. Maniscalco, *EPL* **111**, 50006 (2015).
- [20] M. M. Wolf, J. Eisert, T. S. Cubitt, and J. I. Cirac, *Phys. Rev. Lett.* **101**, 150402 (2008).
- [21] H.-P. Breuer, E.-M. Laine, and J. Piilo, *Phys. Rev. Lett.* **103**, 210401 (2009).
- [22] A. Rivas, S. F. Huelga, and M. B. Plenio, *Phys. Rev. Lett.* **105**, 050403 (2010).
- [23] S. Luo, S. Fu, and H. Song, *Phys. Rev. A* **86**, 044101 (2012).
- [24] S. Lorenzo, F. Plastina, and M. Paternostro, *Phys. Rev. A* **88**, 020102(R) (2013).
- [25] B. Bylicka, D. Chruściński, and S. Maniscalco, *Sci. Rep.* **4**, 5720 (2014).
- [26] B.-H. Liu, L. Li, Y.-F. Huang, C.-F. Li, G.-C. Guo, E.-M. Laine, H.-P. Breuer, and J. Piilo, *Nat. Phys.* **7**, 931934 (2011).
- [27] C.-F. Li, J.-S. Tang, Y.-L. Li, and G.-C. Guo, *Phys. Rev. A* **83**, 064102 (2011).
- [28] S. Cialdi, D. Brivio, E. Tesio, and M. G. A. Paris, *Phys. Rev. A* **83**, 042308 (2011).
- [29] J.-S. Tang, C.-F. Li, Y.-L. Li, X.-B. Zou, G.-C. Guo, H.-P. Breuer, E.-M. Laine, and J. Piilo, *EPL* **97**, 10002 (2012).
- [30] A. Chiuri, C. Greganti, L. Mazzola, M. Paternostro, and P. Mataloni, *Sci Rep.* **2**, 968 (2012).
- [31] J. Jin, V. Giovannetti, R. Fazio, F. Sciarrino, P. Mataloni, A. Crespi, and R. Osellame, *Phys. Rev. A* **91**, 012122 (2014).
- [32] A. Orioux, A. D'Arrigo, G. Ferranti, R. Lo Franco, G. Benenti, E. Paladino, G. Falci, F. Sciarrino, and P. Mataloni *Sci Rep.* **5**, 8575 (2015).
- [33] N. K. Bernardes, A. Cuevas, A. Orioux, C. H. Monken, P. Mataloni, F. Sciarrino, and M. F. Santos, *Sci Rep.* **5**, 17520 (2015).
- [34] S. Cialdi, M. A. C. Rossi, C. Benedetti, B. Vacchini, D. Tamascelli, S. Olivares, and M. G. A. Paris, *Appl. Phys. Lett.* **110**, 081107 (2017).
- [35] T. J. G. Apollaro, C. Di Franco, F. Plastina, and M. Paternostro, *Phys. Rev. A* **83**, 032103 (2011).
- [36] S. Lorenzo, F. Plastina, and M. Paternostro, *Phys. Rev. A* **84**, 032124 (2011).
- [37] P. Haikka, S. McEndoo, G. De Chiara, G. M. Palma, and S. Maniscalco, *Phys. Rev. A* **84**, 031602(R) (2011).
- [38] A. Sindona, J. Goold, N. Lo Gullo, S. Lorenzo, and F. Plastina, *Phys. Rev. Lett.* **111**, 165303 (2013).
- [39] M. Cetina, M. Jag, R. S. Lous, J. T.M. Walraven, R. Grimm, R. S. Christensen, and G. M. Bruun, *Phys. Rev. Lett.* **115**, 135302 (2015).
- [40] M Cetina, M. Jag, R. S. Lous, I. Fritsche, J. T. M. Walraven, R. Grimm, J. Levinsen, M. M. Parish, R. Schmidt, M. Knap, and E. Demler, *Science* **354**, 96 (2016).
- [41] D. Jaksch, C. Bruder, J. I. Cirac, C. W. Gardiner, and P. Zoller, *Phys. Rev. Lett.* **81**, 3108 (1998).
- [42] I. Bloch, J. Dalibard, and, W. Zwerger, *Rev. Mod. Phys.* **80**, 885 (2008).
- [43] M. A. Cazalilla, R. Citro, T. Giamarchi, E. Orignac, and M. Rigol, *Rev. Mod. Phys.* **83**, 1405 (2011).
- [44] M. Greiner, O. Mandel, T. Esslinger, T. W. Hnsch, and I. Bloch, *Nature* **415**, 39-44 (2002).
- [45] T. D. Kühner and H. Monien, *Phys. Rev. B* **58**, 14741(R) (1998).
- [46] P. Haikka, J. Goold, S. McEndoo, F. Plastina, and S. Maniscalco, *Phys. Rev. A* **85**, 060101(R) (2012).
- [47] M. Borrelli, P. Haikka, G. De Chiara, and S. Maniscalco, *Phys. Rev. A* **88**, 010101(R) (2013).
- [48] I. Bloch, *Nat. Phys.* **1**, 23-30 (2005).
- [49] D. van Oosten, P. van der Straten, and H. T. C. Stoof, *Phys. Rev. A* **63**, 053601 (2001).
- [50] S. D. Huber, E. Altman, H. P. Buchler, and G. Blatter, *Phys.*

- Rev. B, **75**, 085106 (2007).
- [51] P. Barmettler, D. Poletti, M. Cheneau, and C. Kollath, *Phys. Rev. A* **85**, 053625 (2012).
- [52] A. Recati, P. O. Fedichev, W. Zwerger, J. von Delft, and P. Zoller, *Phys. Rev. Lett.* **94**, 040404 (2005).
- [53] M. A. Cirone, G. De Chiara, G. M. Palma, and A. Recati, *New J. Phys.* **11**, 103055 (2009).
- [54] F. Cosco, M. Borrelli, F. Plastina, and S. Maniscalco, *Phys. Rev. A* **95**, 053620 (2017).
- [55] S. Ospelkaus, C. Ospelkaus, O. Wille, M. Succo, P. Ernst, K. Sengstock, and K. Bongs, *Phys. Rev. Lett.* **96**, 180403 (2006).
- [56] J. Catani, G. Barontini, G. Lamporesi, F. Rabatti, G. Thalhammer, F. Minardi, S. Stringari, and M. Inguscio, *Phys. Rev. Lett.* **103**, 140401 (2009).
- [57] D. McKay, and B. DeMarco, *New J. Phys.* **12**, 055013 (2010).
- [58] S. Will, T. Best, S. Braun, U. Schneider, and I. Bloch, *Phys. Rev. Lett.* **106**, 115305 (2011).
- [59] N. Spethmann, F. Kindermann, S. John, C. Weber, D. Meschede, and A. Widera, *Phys. Rev. Lett.* **109**, 235301 (2012).
- [60] J. Catani, G. Lamporesi, D. Naik, M. Gring, M. Inguscio, F. Minardi, A. Kantian, and T. Giamarchi, *Phys. Rev. A* **85**, 023623 (2012).
- [61] T. H. Johnson, F. Cosco, M. T. Mitchison, D. Jaksch, and S. R. Clark, *Phys. Rev. A* **93**, 053619 (2016).
- [62] T. B. Batalhão, A. M. Souza, L. Mazzola, R. Auccaise, R. S. Sarthour, I. S. Oliveira, J. Goold, G. De Chiara, M. Paternostro, and R. M. Serra, *Phys. Rev. Lett.* **113**, 140601 (2014).
- [63] H. P. Breuer and F. Petruccione, *The Theory of Open Quantum Systems*, (Oxford University Press, Oxford, 2007).
- [64] T. J. G. Apollaro, S. Lorenzo, C. Di Franco, F. Plastina, and M. Paternostro, *Phys. Rev. A* **90**, 012310 (2014).
- [65] S. Wissmann, A. Karlsson, E.-M. Laine, J. Piilo, and H.-P. Breuer, *Phys. Rev. A* **86**, 062108 (2012).
- [66] S. Lorenzo, F. Plastina, and M. Paternostro, *Phys. Rev. A* **87**, 022317 (2013).
- [67] S. Lorenzo, F. Lombardo, F. Ciccarello, and G. M. Palma, *Sci. Rep.* **7**, 42729 (2017).
- [68] J. Schachenmayer, L. Pollet, M. Troyer, and A. J. Daley, *Phys. Rev. A* **89**, 011601 (2014); J. Schachenmayer, L. Pollet, M. Troyer, and A. J. Daley, *EPJ Quantum Technology* **2015** **2**:1.
- [69] G. Vidal, *Phys. Rev. Lett.* **93**, 040502 (2004).
- [70] Discrepancies between the analytical models and numerical computation, for values of U/J allowing for a direct comparison, arise from two key differences. The first is the dimension of the Hilbert space of the gas; while in the tDMRG approach local Fock states up to $n = 5$ are allowed, the fermionic model introduced above for the strongly interacting gas only includes $n = 0, 1, 2$. Second, unlike the quasi-exact tDMRG method, the analytical results rely on a perturbative approach in deriving the open dynamics of the impurity. Despite such differences, a good agreement between analytical and numerical results is found.
- [71] T. I. D. Kühner, S. R. White, and H. Monien, *Phys. Rev. B* **61**, 12474 (1998).
- [72] A. Luchli, and C. Kollath, *J. Stat. Mech.* P05018 (2008).
- [73] M. Pino, J. Prior, A. M. Somoza, D. Jaksch, and S. R. Clark, *Phys. Rev. A* **86**, 023631 (2012).
- [74] J. P. Ronzheimer, M. Schreiber, S. Braun, S. S. Hodgman, S. Langer, I. P. McCulloch, F. Heidrich-Meisner, I. Bloch, and U. Schneider, *Phys. Rev. Lett.* **110**, 205301 (2013).
- [75] S. Trotzky, Y.-A. Chen, A. Flesch, I. P. McCulloch, U. Schollwöck, J. Eisert, and I. Bloch, *Nat. Phys.* **8**, 325330 (2012).
- [76] The Bogoliubov angles are $\theta_k = \arctan[-2i\Delta_k/(E_k^d + E_k^h)]$, with $E_k^d = -2J(\bar{n} + 1)\cos k + U/2$, $E_k^h = -2J\bar{n}\cos k + U/2$, $\Delta_k = 2iJ\sqrt{\bar{n}(\bar{n} + 1)}\sin k$.
- [77] The energies of the superfluid excitations are given by $\omega_k = \sqrt{4JU n_0(1 - \cos k) + 4J^2(1 - \cos k)^2}$. The energies of the quasi-particles in the doublon/holon description are $\omega_k^{d/h} = \mp J \cos k + \Omega_k$, with $\Omega_k = \frac{1}{2} \sqrt{(E_k^d + E_k^h)^2 + 4|\Delta_k|^2}$.